Effect of co-substitution on the electrocatalytic properties of Ni1.5Fe1.5O4 for oxygen evolution in alkaline solutions.

SINGH, N.K., YADAV, R., YADAV, M.K. and FERNANDEZ, C.

2017

Effect of Co-substitution on the Electrocatalytic Properties of $Ni_{1.5}Fe_{1.5}O_4$ for Oxygen Evolution in Alkaline Solutions

N.K. Singh[1,*], Ritu Yadav[1], M.K. Yadav[1] and Carlos Fernandez[2]

[1]Department of Chemistry, Faculty of Science, University of Lucknow, Lucknow –226007, India
[2]School of Pharmacy and Life Sciences, Robert Gordon University, Aberdeen, AB10 7GJ Scotland, UK

Abstract: *Some ternary ferrites having composition $Co_xNi_{1.5-x}Fe_{1.5}O_4$ ($0.0 \leq x \leq 1.25$) have been synthesized by NH_4OH co-precipitation method at 11.5 pH. Materials, so obtained, were tested for their electrocatalytic properties towards oxygen evolution reaction (OER) in the form film on Ni-support in alkaline solution. The study showed that the electrocatalytic properties the material increased with partial substitution of Co for Ni in the base oxide ($Ni_{1.5}Fe_{1.5}O_4$). The value being highest with 1.25 mol Co-substitution. At E = 850 mV vs Hg/HgO in 1M KOH at 25 ºC, the electrode showed apparent current density 137.1 mA cm^{-2}, which is about 2.5 times higher than the base oxide. The Tafel slope values were ranged between 53-90 mV $decade^{-1}$. A pair of redox peak, an anodic (E_{Pa} = 522±28 mV) and corresponding cathodic (E_{Pc}= 356±9 mV), was observed in the cyclic voltammetry (CV) study of the material. The thermodynamic parameters namely, standard apparent electrochemical enthalpy of activation ($\Delta H_{el}^{*\neq}$), standard enthalpy of activation ($\Delta H^{*\neq}$) and standard entropy of activation ($\Delta S^{*\neq}$) for the oxygen evolution reaction (OER) have also been determined by recording anodic polarization curve in 1M KOH. The value of $\Delta H_{el}^{*\neq}$ was observed to be almost similar with each oxide electrode. The $\Delta S^{*\neq}$ values were highly negative and ranged between ~ -165 and ~ -207 J deg^{-1} mol^{-1}. Phase and morphology of materials have been investigated by using physical techniques X-ray diffraction, infrared spectroscopy (IR) and scanning electron microscope (SEM), respectively.*

Keywords: Co-precipitation; XRD; SEM; Electrocatalysis; Oxygen evolution; activation energy

1. INTRODUCTION

Spinel-ferrites are known to be the best catalytic material and have fabulous biological [1-3] and technological applications [4, 5]. These materials have been very much useful in various heterogeneous catalytic reaction such as for synthesis of ammonia [6], production of chlorate from chlorine [7], selective oxidation of butane [8], decomposition of ammonia [9] etc. over the past half century. Ferrospinels have also been found to be good electrocatalysts for electrolytic evolution of oxygen in alkaline solutions. However, results showed that materials obtained at higher temperature like thermal decomposition [10-15] and freeze-drying [16-18] have low electrocatalytic activity with high overpotentials. It is noteworthy that the electrocatalytic properties of materials strongly dependent on their interfacial properties, which can be improved by using suitable method of preparation, precursors, temperature

and metal ions substitution. During past few decades, various types of binary [20-32] and some ternary [33-38] spinel oxides have been studied for their electrocatalytic properties towards oxygen evolution reaction in alkaline medium. Results showed that ternary oxides exhibited better electrocatalytic activity as compared to binary oxides.

Mendonca et al. [33] used standard ceramic powder method and obtained ternary cobalt ferrites on partial substitution of Ni or Mn for Fe at B-site of the spinel oxide. They reported that Fe is more easily substituted by Mn in comparison to Ni and maintained the cubic phase till 60% of Mn. However, Ni-substituted oxide showed better electrocatalytic activity. Similar electrocatalytic activity has also been observed by Godinho et al. [34] for partially Ni and /or Mn substituted cobalt ferrites. Singh et al. [35-38] also used B-site of the spinel ferrite for the synthesis of ternary oxides and studied the effect of partial substitution of Cr and/or V for Fe on the electrocatalytic properties of the material.

In view of the above study, we developed new ternary ferrites in

*To whom correspondence should be addressed:
Email: nksbhu@yahoo.com; singh_narendra@lkouniv.ac.in
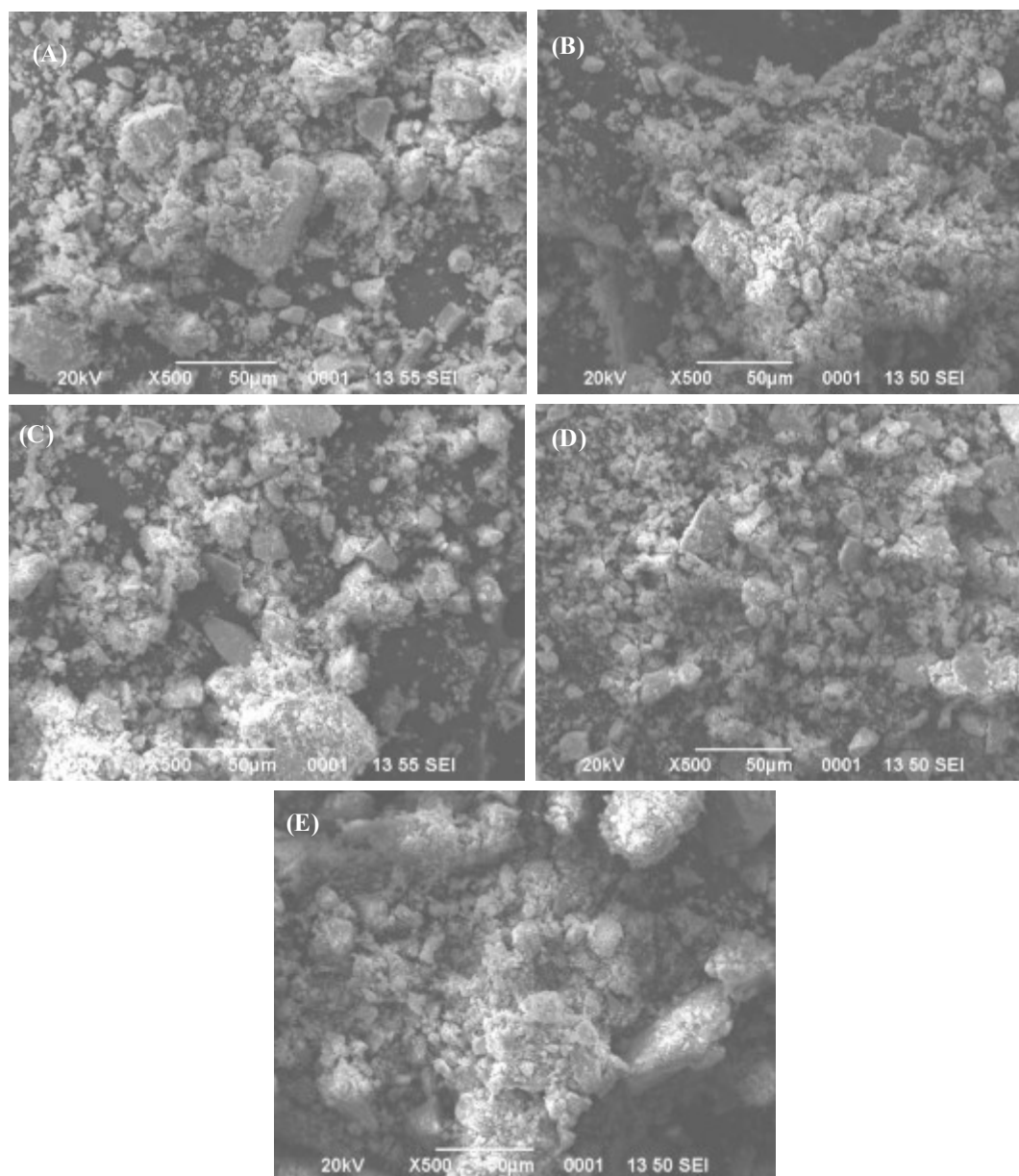Mob.: +91-9451949105

Figure 1. SE Micrographs of oxide powder sintered at 400°C for 5 h; A: $Ni_{1.5}Fe_{1.5}O_4$, B: $Co_{0.5}NiFe_{1.5}O_4$, C: $Co_{0.75}Ni_{0.75}Fe_{1.5}O_4$, D: $CoNi_{0.5}Fe_{1.5}O_4$, E: $Co_{1.25}Ni_{0.25}Fe_{1.5}O_4$.

which cobalt is partially substituted for A-site's Ni of the $Ni_{1.5}Fe_{1.5}O_4$ by using low temperature NH_4OH co-precipitation and studied their electrocatalytic properties for oxygen evolution reaction in alkaline medium. Results, so obtained are summarized and presented in this paper.

2. EXPERIMENTAL

Spinel-type ternary oxides of Co, Ni and Fe having general composition $Co_xNi_{1.5-x}Fe_{1.5}O_4$ ($0.0 \leq x \leq 1.25$) were prepared by co-precipitation method at pH = 11.5. In each synthesis, as per requirement of the particular oxide, stoichiometric quantity of cobalt chloride (purified, Merck 98%), nickel chloride (purified, Merck 97%) and ferric chloride (purified, Merck 97%) were dissolved in 100 ml

double distilled water. To this solution, NH_4OH (25%, Fischer) was added drop wise with constant stirring till the pH of the medium reached to 11.5. The precipitate, so obtained, was filtered and washed with double distilled water till free from chloride ions and finally dried at 100 °C for 24 hrs. In order to get the desired oxide, the dried precipitate was crushed into fine powder in an agate pastel mortar and then sintered at 400 °C for 5hrs in PID controlled electrical furnace (Asco, India).

The materials, so prepared, were characterized by some physico-chemical techniques. The phase and purity of the material was confirmed by X-Ray diffraction (Bruker D-8 advanced series-2 diffractometer using Cu-$K\alpha_1$ as the radiation source; $\lambda = 1.54056$ Å) and IR (FT-IR Thermoscientific; Nicole-6700), respectively.
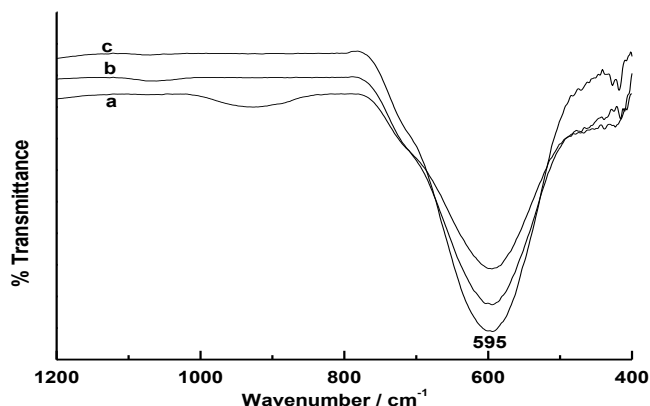
Effect of Co-substitution on the Electrocatalytic Properties of $Ni_{1.5}Fe_{1.5}O_4$ for Oxygen Evolution in Alkaline Solutions / J. New Mat. Electrochem. Systems

117

Figure 2. IR Spectra of $Co_xNi_{1.5-x}Fe_{3-x}O_4$ sintered at 400°C for 5 h; (a) x = 0.5 mol, (b) x = 0.75 mol, (c) x = 1.0 mol.

Figure 3. XRD powder patterns of $Co_xNi_{1.5-x}Fe_{3-x}O_4$, sintered at 400 °C for 5 h; (a) x = 0 mol, (b) x = 0.5 mol, (c) x = 1.0 mol

The Scanning electron microscope (SEM; JEOL JSM 6490) was used to know the morphology and texture of the oxide in the form of powder. All electrochemical studies namely, Cyclic voltammogram (CV) and anodic polarization study, have been carried out in a three-electrode single compartment glass cell using an electrochemical impedance system (Gamry Reference 600 ZRA) provided with potentiostat/galvanostat and a corrosion and physical electrochemistry software installed in the personal computer (PC) system (hp). For the purpose, materials were first transformed in the form of film electrode on a pre-treated Ni-support (Sigma-Aldrich, 99.9%) by an oxide slurry painting method [39]. The preparation of slurry and electrical contact with the oxide film to make the electrode have been performed in the similar way as described in literature [39]. The oxide electrode, so prepared, was used as working electrode. The reference and auxiliary (counter) electrodes were Hg/HgO in 1 M KOH (E° = 0.098 V vs NHE) and pure Pt-foil of geometrical surface area (~2 cm^2), respectively. The potential given in the text for each oxide electrode was measured with respect to Hg/HgO/1 M KOH. The reference electrode was connected to the cell solution through the Luggin capillary (the KCl/Agar-Agar salt bridge) for minimization any resistance appeared by the electrolytic solution.

3. RESULTS AND DISCUSSION

3.1. SEM, IR and XRD Studies

Scanning electron micrographs (SEM) of Co-substituted nickel ferrite oxide powder sintered at 400°C, 5 hrs are shown in Fig. 1(A-E) at magnification ×500. Morphology of each oxide powder was found to be similar and showed almost cloudy appearance along with some aggregates. The distribution of some oxide particles has also been observed in each micrograph.

Infrared (IR) spectra of $Co_xNi_{1.5-x}Fe_3O_4$ (0.5 ≤ x ≤ 1.25) in the form of powder have been recorded over the wave number range 4000-400 cm^{-1}. In order to avoid complexity in presentation, only spectra for x = 0.5, 0.75 & 1.0 in the frequency range 1200-400 cm^{-1} is shown in Fig. 2. The observed strong absorption band at ~ 595 cm^{-1} in figure 2 indicated characteristic peak of spinel ferrite [40-42].

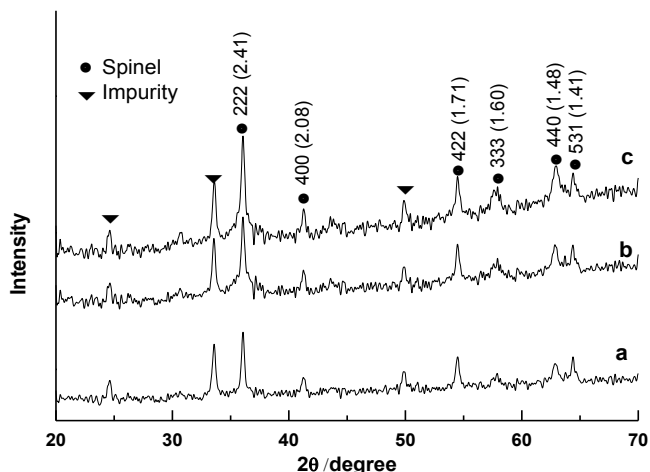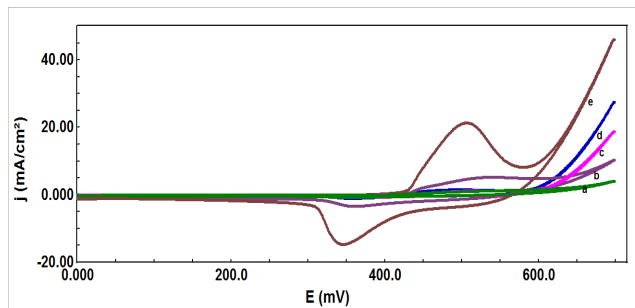The powder X-ray diffraction pattern of the material with x = 0,

Figure 4. Cyclic voltammogram of $Ni/Co_xNi_{1.5-x}Fe_{1.5}O_4$ (0.0 ≤ x ≤ 1.25) electrodes at 20 mV sec^{-1} scan rates in 1M KOH (25°C). a: $Ni_{1.5}Fe_{1.5}O_4$, b: $Co_{0.75}Ni_{0.75}Fe_{1.5}O_4$, c: $CoNi_{0.5}Fe_{1.5}O_4$, d: $Co_{0.5}NiFe_{1.5}O_4$, e: $Co_{1.25}Ni_{0.25}Fe_{1.5}O_4$

0.5 and 1.0, prepared at 400°C, 5 hrs was recorded between 2θ = 20 to 70°. The representative patterns, so obtained, are given in Fig. 3. The observed 2θ and the corresponding d values of the diffracted lines, as shown in figure 3, well matched with JCPDS ASTM file 44-1485 and follow cubic crystal geometry. The diffraction lines corresponding to d values 1.84, 2.69 and 3.68 Å indicate the formation of some additional phases of Fe_2O_3 (JCPDS ASTM Card 01-1053) as impurities. The crystallite size of the material as estimated by using Scherrer formula [43] was found to be 32, 28 and 26 nm with x = 0, 0.5 and 1.0mol, respectively.

3.1. Cyclic Voltammetry

Cyclic voltammograms of each oxide electrode, recorded in 1 M KOH at 25 °C between the potential region 0.0-0.7V, at the scan rate of 20 mVsec^{-1} are shown in Fig 4. Voltammograms of each catalyst were found to be similar and exhibited a pair of redox peaks; one anodic and corresponding cathodic between scanned potential region. Values of corresponding anodic peak potential (E_{Pa}), cathodic peak potential (E_{Pc}), peak potential difference (ΔE_P) and formal redox potential (E°), as given in Table 1, were estimat-
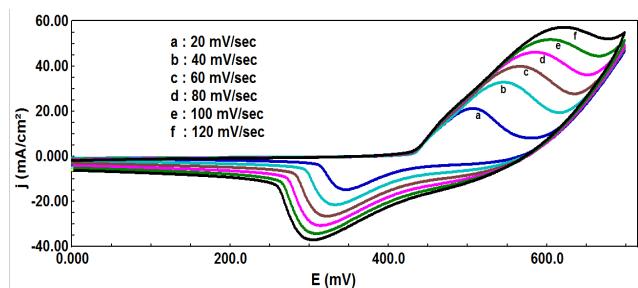
Figure 5. Cyclic voltammograms of the Ni/$Co_{0.5}NiFe_{1.5}O_4$ film electrode at different scan rates in 1M KOH (25°C).
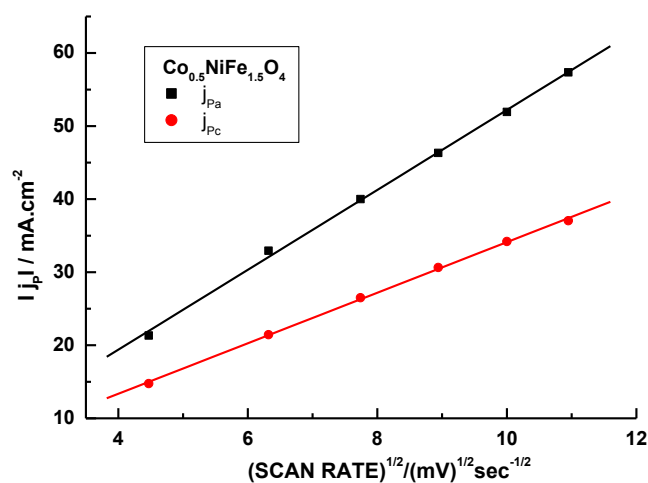

Figure 6. Plot of $|j_P|$ vs. (scan rate)$^{1/2}$ for the $Co_{0.5}NiFe_{1.5}O_4$ film on Ni in 1M KOH (25 °C)

Figure 7. Plot of voltammetric charge (q) vs. (scan rate)$^{-1/2}$ for ferrite film electrodes on Ni (25 °C).
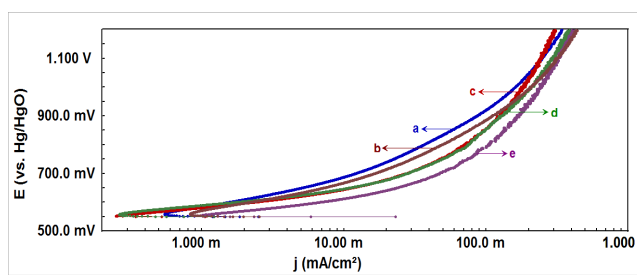
Figure 8. Anodic polarization curves for Ni/$Co_xNi_{1.5-x}Fe_{1.5}O_4$ (0.0 ≤ x ≤ 1.25) in 1M KOH (25°C); scan rate:0.2 mVsec^{-1}. a: $Ni_{1.5}Fe_{1.5}O_4$, b: $Co_{0.75}Ni_{0.75}Fe_{1.5}O_4$, c: $Co_{0.5}NiFe_{1.5}O_4$, d: $CoNi_{0.5}Fe_{1.5}O_4$, e: $Co_{1.25}Ni_{0.25}Fe_{1.5}O_4$

ed from the cyclic voltammetric curves and found to be in the range between 522 ± 28 mV, 356 ± 9 mV, 165 ± 33 mV and 441 ± 15 mV, respectively. The observed values of anodic peak potential and cathodic peak potential correspond to the redox potential of Ni(II)/Ni(III), which might undergo surface conversion [44] with the contact of electrolyte as given by the equation.
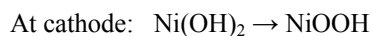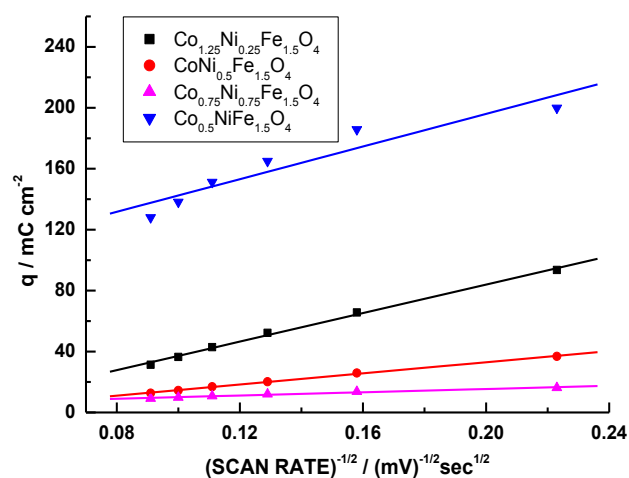
At anode: $NiOOH \rightarrow Ni(OH)_2$

At cathode: $Ni(OH)_2 \rightarrow NiOOH$

Table 1. Values of the cyclic voltammetric parameters of Ni/$Co_xNi_{1.5-x}Fe_{1.5}O_4$ (0.0 ≤ x ≤ 1.25) in 1M KOH at 25 °C (scan rate = 20 mV sec^{-1}).

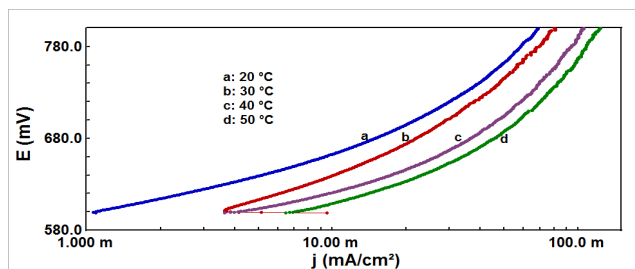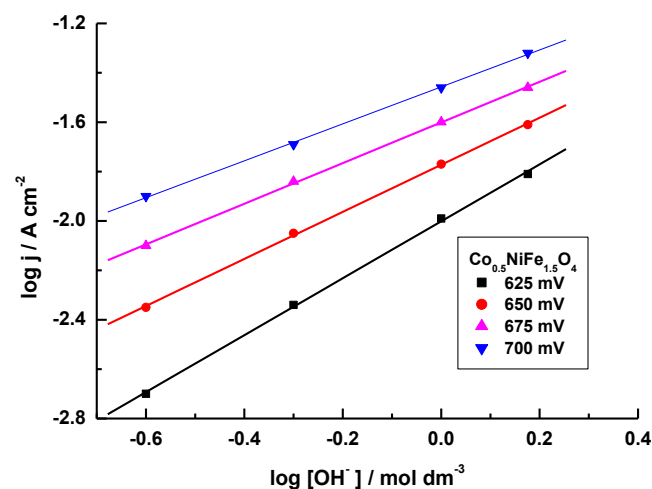| Electrode	E_{Pa} /mV	E_{Pc} /mV	ΔE_P /mV	$E° = (E_{Pa} + E_{Pc})/2$ /mV
$Ni_{1.5}Fe_{1.5}O_4$	550	362	188	456
$Co_{0.5}NiFe_{1.5}O_4$	550	352	198	451
$Co_{0.75}Ni_{0.75}Fe_{1.5}O_4$	494	362	132	428
$CoNi_{0.5}Fe_{1.5}O_4$	525	364	161	445
$Co_{1.25}Ni_{0.25}Fe_{1.5}O_4$	505	347	158	426

It is also well known [20, 45] that the oxides prepared at low temperature are observed to be hydrophilic in nature and undergo rapid hydration in aqueous solution, resulting the wetting of whole catalytic film thickness.

The CV curve of each oxide electrodes was also recorded between the same potential regions at varying scan rates. A representative curve for $Co_{0.5}NiFe_{1.5}O_4$ is shown in Fig. 5. The nature of CV curve observed at different scan rates was almost similar to that found at the scan rate of 20 mV sec^{-1}. However, position of both anodic and cathodic peaks shifted towards either side as the scan rate is increased from 20 to 120 mV sec^{-1}. This indicates the quasi-reversible nature of the redox couple.

The variation of anodic and cathodic peak current with scan rate was determined by constructing a plot, peak current ($|j_p|$) vs square root of scan rate, for each oxide electrode. A representative plot for $Co_{0.5}NiFe_{1.5}O_4$ is shown in Fig. 6. The voltammetric charge (q) vs (scan rate)$^{-1/2}$ (Fig. 7) was also constructed for each oxide electrodes. The linearity observed in the figure 7 indicates that the surface redox process is diffusion controlled [46].

3.2. Electrocatalytic activity

The electrocatalytic activity of materials prepared *in situ* was determined by recording iR-uncompensated anodic polarization curve (E *vs* log j) in 1M KOH at 25 °C at the scan rate of 0.2 mV
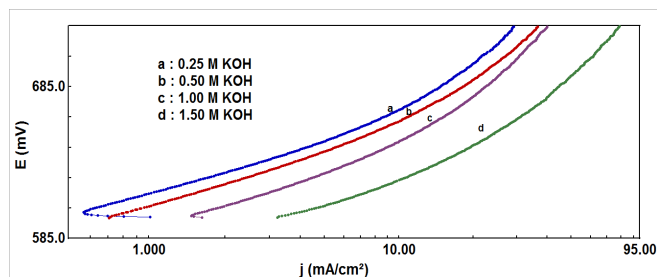
Figure 9. Anodic polarization curve for Co$_{0.5}$NiFe$_{1.5}$O$_4$ film on Ni at varying KOH concentrations (m = 1.5) at 25°C.

Figure 11. Tafel plots for oxygen evolution on the Co$_{0.5}$NiFe$_{1.5}$O$_4$ film on Ni at different temperatures in 1 M KOH

Figure 10. Plot of log j vs log [OH$^-$] at different applied potential for Co$_{0.5}$NiFe$_{1.5}$O$_4$ film electrode on Ni at 25°C.

Co$_{1.25}$Ni$_{0.25}$Fe$_{1.5}$O$_4$ (j$_a$ = 137.1 mA cm^{-2}) > Co$_{0.5}$NiFe$_{1.5}$O$_4$ (j$_a$ = 96.9 mA cm^{-2}) ≈ CoNi$_{0.5}$Fe$_{1.5}$O$_4$ (j$_a$ = 99.4 mA cm^{-2}) > Co$_{0.75}$Ni$_{0.75}$Fe$_{1.5}$O$_4$ (j$_a$ = 76.4 mA cm^{-2}) > Ni$_{1.5}$Fe$_{1.5}$O$_4$ (j$_a$ = 58.3 mA cm^{-2})

This indicates that the requisite amount of Co-substitution into the nickel ferrite modifies the geometrical and electrocatalytic activity of the oxide. The order of reaction was determined by recording anodic polarization curve in different KOH concentrations (0.25-1.5M). During the experiment, the ionic strength (μ = 1.5) of the electrolytic solution was kept constant by adding KNO$_3$ an inert electrolyte. A representative curve is shown in Fig. 9. From the data of the polarization curve obtained at different concentration, a plot, log j vs. log [OH$^-$] was constructed. A representative plot for Co$_{0.5}$NiFe$_{1.5}$O$_4$ at different applied potentials is shown in Fig. 10. The reaction order as given in table 2, was calculated from the slope of the straight line and found to be approximately unity in each case. The values of Tafel slope (b) and reaction order (p) indicate that the oxide electrodes follow two different mechanistic paths, such as 2.3RT/F (~ 60 mV decade^{-1}) and 3×2.3RT/2F (~ 90 mV decade^{-1}).

The activation energy and other thermodynamic parameters of the oxide electrode were determined by recording the anodic polarization curve in 1M KOH at varying temperatures (20°-50°C). The representative polarization curve for Co$_{0.5}$NiFe$_{1.5}$O$_4$ is shown in Fig. 11. During the experiment, the temperature of the reference was maintained constant at 25°C. From the data, Arrhenius plot, log j vs 1/T, was constructed and a representative plot for Co$_{0.5}$NiFe$_{1.5}$O$_4$ at different applied potential is shown in the Fig. 12. The activation energy was estimated by measuring the slope of the straight lines. Also, the figure 12 indicates that the value of activa-

sec^{-1}. The polarization curves, so obtained, for each oxide electrode are shown in Fig. 8. The electrode kinetic parameters such as Tafel slope and electrocatalytic activity in terms of current density at a fixed potential as well as in terms of potential at a constant current density were estimated from the polarization curve and given in Table 2. The table shows that among all electrocatalysts, Co$_{1.25}$Ni$_{0.25}$Fe$_{1.5}$O$_4$ was found to be the electrocatalytically most active, while the base oxide (Ni$_{1.5}$Fe$_{1.5}$O$_4$) was the least active one. Values of Tafel slope were ranged between 53-90 mV decade^{-1}. Based on the apparent current density data, at a fixed potential of 850 mV, the oxide catalyst showed the order:

Table 2. Electrode kinetic parameters for Ni/Co$_x$Ni$_{1.5-x}$Fe$_{1.5}$O$_4$ (0.0 ≤ x ≤ 1.25) in 1M KOH at 25 °C (scan rate = 0.2 mV sec^{-1})

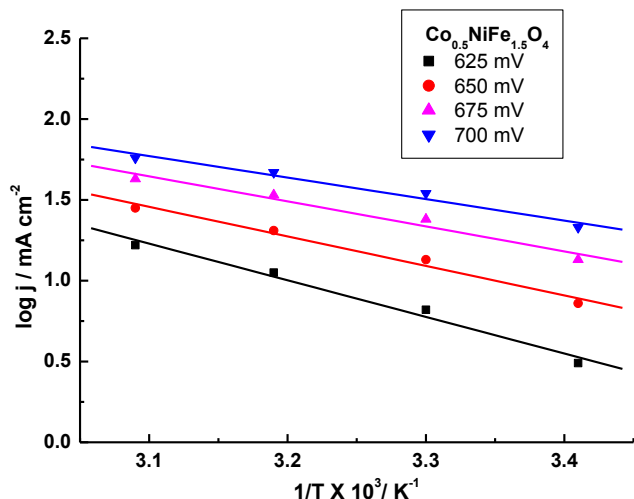| Electrode	Oxide loading (mg/cm^2)	Tafel slope / mVd^{-1}	Order (p)	E/ mV at j (mAcm^{-2})		j (mAcm^{-2}) at E/mV		
				10	100	650	750	850
Ni$_{1.5}$Fe$_{1.5}$O$_4$	3.6	88	1.2	685	919	5.4	23.3	58.3
Co$_{0.5}$NiFe$_{1.5}$O$_4$	4.2	53	0.7	645	850	11.5	47.8	96.9
Co$_{0.75}$Ni$_{0.75}$Fe$_{1.5}$O$_4$	5.8	90	1.2	667	884	7.4	30.3	76.4
CoNi$_{0.5}$Fe$_{1.5}$O$_4$	5.3	55	0.8	647	852	10.9	49.2	99.4
Co$_{1.25}$Ni$_{0.25}$Fe$_{1.5}$O$_4$	6.1	55	1.0	611	792	24.3	75.8	137.1

Figure 12. The Arrhenius plot at different constant applied potentials for $Co_{0.5}NiFe_{1.5}O_4$ in 1 M KOH.

tion energy is decreased as the potential is increased from 625 mV to 700 mV and well satisfied by equation (1). Further, other thermodynamic parameters such as α, $\Delta H_{el}^{o\neq}$, $\Delta H^{o\neq}$ and $\Delta S^{o\neq}$ were calculated by using following relations [36, 47];

$$\Delta H_{el}^{o\#} = \Delta H^{o\#} - \alpha F \eta \tag{1}$$

Where, α (transfer coefficient) = 2.303RT/bF and R, F and T are the gas constant, Faraday constant and absolute temperature, respectively. The Tafel slope (b) is calculated from the polarization curves obtained at different temperatures. η is the overpotential that is $\eta = E - E_{O_2/OH^-}$, where, E and E_{O_2/OH^-} (= 0.303 V vs. Hg/HgO) are the applied potential across the catalyst/ 1 M KOH interface and the theoretical equilibrium Nernst potential in 1 M KOH at 25 °C, respectively.

$$DS^{o\#} = 2.3R [\log j + DH_{el}^{o\#} /2.3RT - \log (nF\omega C_{OH^-})] \tag{2}$$

Where, ω (= $k_B T/h$) is the frequency term and $n = 2$, k_B and h are the Boltamann constant and Plank's constant, respectively.

The estimated values of transfer coefficient (α), standard apparent enthalpy of activation $\Delta H_{el}^{o\#}$, standard enthalpy of activation ($\Delta H^{o\#}$) and entropy of activation ($\Delta S^{o\#}$) are given in Table 3. From table 3, it has been observed that the activation energy calcu-

lated at E = 650 mV for each oxide electrode varied slightly in the range between 38.4 and 46.9 kJ mol⁻¹. The values of entropy of activation ($DS^{o\#}$), as calculated by using equation (2), were found to be highly negative and ranged between -181.1 and -207.2 J deg⁻¹ mol⁻¹. A negative change in the entropy indicates that the disorder of a system has been decreased. The decrease in the negative value of entropy with the substitution of cobalt in the base oxide indicated the decrease in the role of adsorption phenomenon in the electrochemical formation of oxygen thereby increased the oxygen evolution reaction.

4. CONCLUSION

In the present study, Co is partially substituted for Ni in the $Ni_{1.5}Fe_{1.5}O_4$ binary spinel oxide. The results showed that the electrocatalytic activity of the material is increased with increase the Co content in the base oxide except 0.75 mol Co-substitution. At E = 850 mV vs Hg/HgO in 1M KOH at 25 ºC, 1.25 mol Co-substitution showed apparent current density 137.1 mA cm⁻², which is about 2.5 times higher than the base oxide. The Tafel slope values were ranged between 53-90 mV decade⁻¹. Cyclic voltammetric study indicates a pair of redox peak, an anodic (E_{Pa} = 522±28 mV) and corresponding cathodic (E_{Pc} = 356±9 mV), for each oxide electrode. The activation energy calculated at E = 650 mV was observed to be almost similar for each oxide electrode.

REFERENCES

[1] Pulfer S. K., Gallo J. N., Scientific and Clinical Applications of magnetic carriers, Häfeli U., Schütt W., Teller J., Zborowski M., (Plenum Press: New York) 1997, p. 445.

[2] Zarur A. J., Ying J. V., Nature, 403, 65 (2000).

[3] Sousa M. H., Hasmonay E., Depeyrot J., Tourinho F. A., Bacri J. C., Dubosis E., Perzyski R., Raikherb Y. L., Magn J., Mater., 242, 572 (2002).

[4] Raj K., Moskowitz R., J. Magn. Magn. Mater., 85, 233 (1990).

[5] Sepelak V., Baabe D., Mienert D., Schultze D., Krumeich F., Litterst F. J., Becker K. D., Magn Mater, 257, 377 (2003).

[6] Rajaram R. R., Sermon, J. Chem. Soc. Faraday Trans., 81, 2277 (1985).

[7] Trasatti S.,Lodi G., Electrodes of Conductive Metallic Oxides, Part B, edited by Trasatti S. (Elsevier, Amsterdam) 1981, 569.

[8] Harold H. K., Mayfair C. K., Adv. Catal., 33, 159 (1985).

[9] Kota H. M., Katan J., Chim M., Schoenweis, Nature, 203, 1281 (1964).

[10] Tarasevich M. R., Efremov B. N., Electrodes of conductive metallic oxides, Part A, edited by Trasatti S., (Elsevier, Amsterdam), 1980.

[11] Boggio R., Camgati A., Trassati S., J. Appl. Electrochem., 17, 828 (1987).

Table 3. Thermodynamic parameters for O_2 evolution on $Ni/Co_xNi_{1.5-x}Fe_{1.5-x}O_4 (0.0 \leq x \leq 1.25)$ in 1 M KOH.

Electrode	$\Delta H_{el}^{o\neq}$ (kJ mol⁻¹) at E = 650 mV	$-\Delta S^{o\neq}$ (Jdeg⁻¹ mol⁻¹)	α	$\Delta H^{o\neq}$ (kJ mol⁻¹)
$Ni_{1.5}Fe_{1.5}O_4$	38.4	207.2	0.7	59.9
$Co_{0.5}NiFe_{1.5}O_4$	42.7	190.0	0.8	57.9
$Co_{0.75}Ni_{0.75}Fe_{1.5}O_4$	46.9	165.9	1.2	64.6
$CoNi_{0.5}Fe_{1.5}O_4$	44.8	181.4	1.3	80.8
$Co_{1.25}Ni_{0.25}Fe_{1.5}O_4$	44.6	181.1	1.3	71.6

[12]Da Silva L. M., De Faria L. A., Boodts J. F. C., J. Electroanal. Chem., 141, 532 (2002).

[13]Tavares A. C., Cartaxo M. A. M., Da Silva Pereira M., Costa F. M., J. Solid State Electrochem., 5, 57 (2001).

[14]Nikilov I., Darkaoui R., Zhecheva E., Stoyanova R., Dimitrov N., Vitanov T., J. Electroanal Chem., 429, 157 (1997).

[15]Yuh-Shu L., Chi-Chang H., Jen-Chen W., J. Electrochem. Soc., 143(4), 1218 (1996).

[16]Iwakura C., Nishioka M., Tamura H., Nippon Kagaku Kaishi, 7, 136 (1982).

[17]Iwakura C., Honji A., Tamura H., Electrochim. Acta., 26, 1319 (1981).

[18]Rasiyah P., Tseung A. C. C., J. Electrochem. Soc., 130, 365 (1983).

[19]Orehotsky J., Huang H., Davidson C. R., Srinivasan S., J. Electroanal. Chem., 95, 233 (1979).

[20]Singh N. K., Tiwari S. K., Anitha K. L., Singh R. N., J. Chem. Soc. Faraday Trans., 92(13), 2397 (1996).

[21]Bocca C., Barbucci A., Deluchi M., Ceriola G., Int. J. Hydrogen Energy, 24, 21 (1999).

[22]Bocca C., Ceriola G., Magnone E., Barbucci A., Int. J. Hydrogen Energy, 24, 699 (1999).

[23]Baydi M. El., Poillerat G., Rehspringer J. L., Gautier J. L., Koenig J. F., Chartier P., J. Solid State Chem., 109, 281 (1994).

[24]Martin J. L., Vidales de, Martinez Garcia O., Vila E., Rojas R. N., Torralvo M. J., Mat. Res. Bull., 28, 1135 (1993).

[25]Baydi M. El., Tiwari S. K., Singh R. N., Koenig J. F. Poillerat G., J. Solid State Chem., 116, 157 (1995).

[26]Singh N. K., Singh J. P., Singh R. N., Int. J. Hydrogen Energy, 27, 895 (2002).

[27]Svegl F., Orel B., Svegl I. G., Kaucic V., Electrochim. Acta, 45, 4359 (2000).

[28]Singh J. P., Singh N. K., Singh R. N., Int. J. Hydrogen Energy, 24, 433 (1999).

[29]Singh R. N., Singh J. P., Lal B., Singh A., Int. J. Hydrogen Energy, 32, 11 (2007).

[30]Singh N. K., Singh R. N., Ind. J. Chem., 38A, 491 (1999).

[31]Singh R. N., Singh J. P., Singh A., Int. J. Hydrogen Energy, 33, 4260 (2008).

[32]Al-Hoshan M. S., Singh J. P., Al-Mayouf A. M., Al-suhybani A. A., Shaddad M. N., Int. J. Electrochem. Sci., 7, 4959 (2012).

[33]Mendonca M. H., Godinho M. I., Catarino M. A., Da silva Pereira M. I., Costa F. M., Solid State Science, 4, 175 (2002).

[34]Godinho M. I., Catarino M. A., Da silva Pereira M. I., Mendonca M. H., Costa F. M., Electrochim. Acta, 47, 4307 (2002).

[35]Singh R. N., Singh N. K., Singh J. P., Electrochim. Acta, 47, 3873 (2002).

[36]Singh R. N., Singh N. K., Singh J. P., Balaji G., Gajbhiye N. S., Int. J. Hydrogen Energy, 31, 701 (2006).

[37]Singh R. N., Singh J. P., Lal B., Singh A., Int. J. Hydrogen Energy, 32, (2007).

[38]Anindita, Singh A., Singh R. N., Int. J. Hydrogen Energy, 35, 3243 (2010).

[39]Tiwari S. K., Chartier P., Singh R. N., J. Electrochem. Soc. 142, 148 (1995).

[40]Gillot B., Laarz M., Kacim S., J. Mater. Chem. 7, 827 (1997).

[41]Gillot B., Nivoix V., Kester E., Nusillard O., Villete .C, Tailhades Ph., Rousset A., Mater. Chem. Phys., 48, 111 (1997).

[42]Okasha N., Mater. Chem. Phys., 84, 63 (2004).

[43]Fradette N., Marsan B., J. Electrochem. Soc., 145, 2320 (1998).

[44]Egelund S., Caspersen M., Nikiforov A., Moller P., Int. J. Hydrogen Energy, 41, 10152 (2016).

[45]Trasatti S., in The Electrochemistry of Novel Materials ed. Lipkowski J., Ross P. N., VCH, New York, 1994.

[46]Singh R. N., Tiwari S. K., Singh S. P., Singh N. K., Pollerat G., Chartier P., J. Chem. Soc. Faraday Trans., 92(14), 2593 (1996).

[47]Gileadi E., Electrode Kinetics, (VCH Publishers Inc., New York), 1993 p.151.